



Performance of combined displacement ventilation and cooled ceiling liquid desiccant membrane system in Beirut climate

Mohamad Muslmani, Nesreen Ghaddar & Kamel Ghali

To cite this article: Mohamad Muslmani, Nesreen Ghaddar & Kamel Ghali (2016) Performance of combined displacement ventilation and cooled ceiling liquid desiccant membrane system in Beirut climate, Journal of Building Performance Simulation, 9:6, 648-662, DOI: [10.1080/19401493.2016.1185153](https://doi.org/10.1080/19401493.2016.1185153)

To link to this article: <https://doi.org/10.1080/19401493.2016.1185153>



Published online: 24 May 2016.



Submit your article to this journal [↗](#)



Article views: 254



View related articles [↗](#)



View Crossmark data [↗](#)



Citing articles: 2 View citing articles [↗](#)

Performance of combined displacement ventilation and cooled ceiling liquid desiccant membrane system in Beirut climate

Mohamad Muslmani, Nesreen Ghaddar* and Kamel Ghali

Department of Mechanical Engineering, American University of Beirut, PO Box 11-236 Riad El-Solh, Beirut 11072020, Lebanon

(Received 13 February 2016; accepted 28 April 2016)

The performance of the chilled ceiling (CC) displacement ventilation (DV) systems is constrained by latent load removal capacity and cost of supply air dehumidification to prevent condensation on the ceiling. In this study, a liquid desiccant dehumidification membrane cycle (LDMC) is mathematically modelled to replace the CC and remove directly latent and sensible load from indoor space through the membrane. The desiccant system is coupled with the DV system. An optimized operational strategy is adopted while allowing ceiling temperature to drop to lower values than conventional CC/DV. The optimized LDMC-C/DV system was implemented in an office space in Beirut climate. It was found that decreasing the membrane liquid desiccant temperature resulted in a significant decrease in the total cooling energy of the system, while increasing the solar heating energy of the desiccant regeneration. At optimal set points, a decrease of 49% in energy consumption was observed compared to the conventional CC/DV system.

Keywords: liquid desiccant membrane; displacement ventilation; chilled ceiling; optimization; energy efficiency; indoor air quality

Nomenclature

A	area (m^2)	p	present worth value
c	concentration of water per desiccant (kg_{H_2O}/kg_{CaCl_2})	$P_{chiller}$	chiller capacity (W)
CC	chilled ceiling	PLR	part load ratio
C_p	specific heat ($J/kg\ K$)	PMV	Predicted Mean Vote
d	discount rate	Q_s	Cooling energy needed for supply air (W)
D	diffusion constant of vapour in the pipe wall material (m^2/s)	Q_d	Cooling energy needed for liquid desiccant (W)
DV	displacement ventilation	Q_{DV}	sensible load removed by the DV system (W)
h_c	heat convection coefficient ($W/m^2\ s$)	r_o	external radius of the pipe (m)
h_m	mass convection coefficient (m/s)	r_i	internal radius of the pipe (m)
h_{fg}	latent heat of vaporization of the water (J/kg)	R	CC cooling load to room total load = Q_c/Q_s
h_d	enthalpy of the liquid desiccant solution (J/kg)	T	temperature ($^{\circ}C$)
h_s	enthalpy of supply air (J/kg)	T_a	indoor room ($^{\circ}C$)
K	thermal conductivity ($W/m\ K$)	T_{∞}	ambient temperature ($^{\circ}C$)
L	length of the pipe (m)	T_w	wall temperature ($^{\circ}C$)
LDMC-C/DV	liquid desiccant membrane cycle at the ceiling combined with the DV system	T_c	ceiling temperature ($^{\circ}C$)
\dot{m}	mass rate (kg/s)	T_s	supply air temperature ($^{\circ}C$)
n	number of years	U	resistance coefficient of permeable pipe per unit length
N	number of dehumidification/regeneration pipes	w	humidity ratio (kg_{H_2O}/kg_{dryair})
		w_a	indoor room humidity ratio (kg_{H_2O}/kg_{dryair})
		w_{sol}	the solution equilibrium humidity ratio (kg_{H_2O}/kg_{dryair})

*Corresponding author. Email: farah@aub.edu.lb

Greek letters

ρ	density (kg/m ³)
∞	cost function weighing factor

Subscripts

a	room air
c	heat convection
d	CaCl ₂ and H ₂ O desiccant solution
i	indoor conditions
m	mass convection
s	supply air conditions
o	outdoor conditions
w	wall

1. Introduction

Many studies have focused on new heating ventilation and air-conditioning (HVAC) systems that improve thermal comfort and reduce energy consumption. Among these systems is the displacement ventilation (DV) system. In DV, the supply fresh air enters the room at the floor level and displaces the warmer air that rises due to buoyancy effect to reach the ceiling level where they are exhausted (Jiang, Chen, and Moser 1992; Yuan, Chen, and Glicksman 2001). To prevent thermal drafts at the occupied level and ensure thermal comfort, DV system supply air temperature should not be less than 18°C and velocities should not exceed 0.2 m/s (ASHRAE 2009). For this reason, the maximum load that can be removed from the occupied zone by a DV system is approximately 40 W/m² of floor area (Yuan, Chen, and Glicksman 2001). Behne (1999) reported that using chilled ceiling (CC) with the DV system would increase the cooling load limit to 100 W/m² of floor area. Due to their energy transfer mostly by radiation, CC systems provide better thermal comfort, and reduce energy consumption and noise (Joege and Armando 2002). Increasing the portion of the load carried by the CC is reported to enhance the indoor thermal comfort (Keblawi et al. 2009). However, this may be impractical with the conventional CC/DV systems, since CC systems are constrained with the problem of condensation of water vapour. If the CC panel temperature drops below the dew point temperature of the space, condensation takes place on the panel which limits the ceiling temperature to always be above the room air dew point.

To prevent condensation, humidity is removed from the air at the supply section. The conventional way of removing moisture is by cooling the supply air to a temperature below its dew point temperature to condense the excess moisture and then reheating it to the adequate supply air temperature (Xiao, Gaoming, and Xiaofeng 2011). But this is not an energy-efficient method due to the additional sub-cooling and reheat energy needed (Xiao, Gaoming, and Xiaofeng 2011; Wang et al. 2013). Researches considered sustainable dehumidification techniques by using

desiccant technology as a passive method for dehumidification of supply air (Hao et al. 2007; Fauchoux et al. 2010; Mohammad et al. 2013; Wang, Zhang, and Xia 2013; Abdel-Salam, Ge, and Simonson 2014; Ge et al. 2014; Woods 2014; Abdel-Salam and Simonson 2016). However, a direct contact takes place between the strong desiccant solution and the supply air during dehumidification, which leads to carryover of hazardous salts to the ventilation system causing negative impacts related to health issues and corrosion problems (Studak and Peterson 1988).

To overcome the previous problems with desiccant dehumidification systems, researchers have implemented liquid desiccant membranes to cool and dehumidify air without direct contact with the desiccant (Fauchoux, Simonson, and Torvi 2008, 2009; Crofoot and Harrison 2012; Cheng and Zhang 2013; Eldeeb, Fauchoux, and Simonson 2013; Ge et al. 2013; Abdel-Salam et al. 2016). The membranes are impermeable to liquid desiccant but permeable to water vapour. A membrane constructed of circular pipes was modelled and experimentally validated by Keniar, Ghali, and Ghaddar (2015) for direct indoor dehumidification. This dehumidification methodology eliminates the danger of transferring hazardous liquid desiccant to the indoor air since there is no direct contact between the dehumidifying air and the liquid desiccant. The solar-regenerated liquid desiccant membrane might be an effective system when combined with a DV system and used as a CC to enhance the indoor comfort with low ceiling temperatures without the presence of condensation.

The performance of the liquid desiccant membrane CC combined with the DV system (LDMC-C/DV) involves the simultaneous operation of two subsystems with multiple variables (air and desiccant flow rates, supply air temperature, and desiccant inlet flow temperature) to be controlled under dynamic loading unlike conventional systems. Optimization of the operating parameters and control strategies in conventional CC/DV systems has been used by researchers to minimize the energy consumption and ensure the indoor air quality (IAQ) (Niu, Zhang, and Zuo 2002; Mossolly, Ghali, and Ghaddar 2009; Keblawi, Ghaddar, and Ghali 2011). Mossolly, Ghali, and Ghaddar (2009) showed that using a CC/DV control strategy that varied optimally the CC temperature, DV air supply flow rate, and temperature resulted in more than 15% energy reduction in comparison with single variable control strategy based on varying CC temperature. The supply humidity control in the CC/DV optimized operation systems, however, remained energy-intensive for the prevention of the water vapour condensation on the ceiling (Xiao, Gaoming, and Xiaofeng 2011; Bahman, Rosario, and Rahman 2012). Replacing the CC by liquid desiccant membrane for heat and mass transfer at the indoor space may result in the change of optimal set points for the CC/DV system operation. An optimized operational strategy is needed because the ranges of the operational variables change

when the DV system is combined with the membrane dehumidification ceiling where condensation is no longer a constraint on ceiling temperature. Such optimization of the LDMC-C/DV system has not been studied in the literature.

In this study, a liquid desiccant membrane system is proposed to be used as CC combined with a DV system to provide thermal comfort needs for an office space in Beirut climate. The aim of the work is to study the effect of lowering the CC temperature (lower than the conventional CC/DV system) on the energy consumption of the integrated system while maintaining good IAQ and thermal comfort. In addition, the economic feasibility and hourly performance of the LDMC-C/DV system are compared to a conventional CC/DV air-conditioning system to assess the change in DV and CC loads. The proposed LDMC-C/DV system overcomes the ceiling temperature limitation of conventional CC/DV systems, where lower temperature could be reached in the proposed system without the onset of condensation on the ceiling.

2. LDMC-C/DV system description

The combined LDMC-C/DV system is composed of four main subsystems: the liquid desiccant cycle, the DV system, the parabolic solar collector, and the space thermal model. Figure 1 illustrates the system components. The liquid desiccant cycle includes the indoor dehumidification permeable pipes, outdoor desiccant regeneration permeable pipes, and heat exchangers. The DV system consists of a fan and a cooling coil. The DV air circulation system

circuit is open where 100% fresh air is brought into the space and hence air quality of such a system is high.

The pipes in the system are solid ones except in the regenerator and dehumidifier parts, where the pipes are made of porous material that is permeable to water vapour only, and not to liquid. The cold desiccant flow enters the membrane pipe at (1) picking the moisture and a part of the sensible load from the indoor space and then leaves the membrane at (2), where it is pumped by a pump through the solid piping system. The desiccant is preheated in heat exchanger (A) picking the heat from the liquid leaving the regenerative membrane. After that, the desiccant is heated by the solar energy in exchanger (B) through hot water stored in a tank that is additionally supplemented by a backup auxiliary heater which could be gas fired or electrically heated. Then, the heated desiccant enters the regenerator at (4) to release the absorbed moisture into the ambient air. Before entering the indoor space membrane, the desiccant will be cooled by chilled water supplied by the chiller, through exchanger (C). After that the desiccant enters the dehumidifier again at (1).

In order to heat the liquid desiccant before entering the regenerative membrane, solar energy is used as a heat source. Solar radiation is collected by using parabolic solar panels that will heat a working fluid stored in a storage tank, which in turn will heat the liquid desiccant through heat exchanger (B) before it enters the regenerator, where the regeneration process takes place with ambient external air. If the solar energy is not sufficient to raise the liquid desiccant to the regeneration temperature, an auxiliary heater will be used.

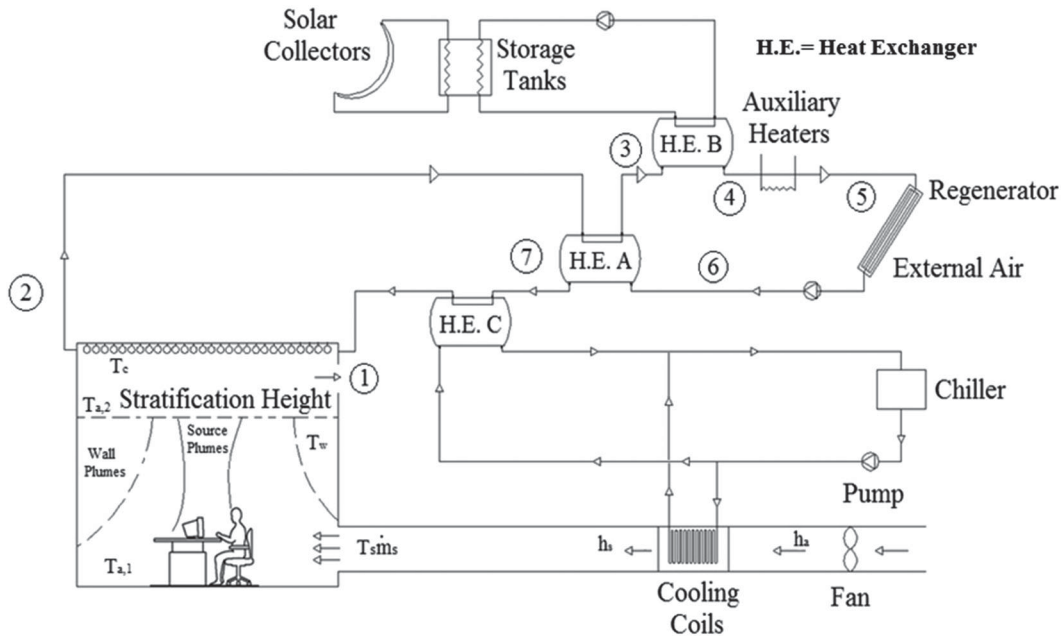


Figure 1. Schematic of the combined LDMC-C/DV system with liquid desiccant cycle.

The chiller is responsible for the removal of the sensible load of the combined system. It provides chilled water to the cooling coil, where the inlet air is cooled to the supply temperature directly, and also provides chilled water to cool the liquid desiccant entering the indoor membrane. The fan supplies the occupied zone with the sufficient amount of inlet air to meet the ventilation and load requirements. For this combined system, several variables are involved in controlling the space thermal comfort and IAQ, which are the supply air temperature, the supply air mass flow rate, and the liquid desiccant temperature at the inlet of the membrane. The supply air temperature, supply air mass flow rate, and liquid desiccant temperature need to be interrelated to each other at each prediction period to provide the desired good IAQ and thermal comfort while minimizing the energy consumption of the system.

In this study, each component of the cycle is modelled independently; then component models are coupled to form an integrated model of the complete cycle. In addition, optimal set points of the control variables are determined to minimize energy consumption while maintaining good IAQ and thermal comfort. A cost function for the system operation is formulated including the electrical cost function and the thermal comfort constraints. The optimization is performed using a genetic algorithm (Mitchell 1997; Wang and Jin 2000) that deals with the following variables:

- (1) The desiccant temperature at the inlet of the membrane (T_1).
- (2) The supply air temperature (T_s).
- (3) The supply air mass flow rate (\dot{m}_s).

The genetic algorithm searches for an optimal value of the variables that varies between a lower and an upper bound in order to minimize energy consumption and maintain thermal comfort and air quality in the occupied space. The combined LDMC-C/DV system has been applied to a case study for an office in Beirut city where its performance is evaluated and compared to that of conventional CC/DV air-conditioning systems.

3. Mathematical modelling

3.1. Liquid desiccant dehumidification cycle

The main component of the liquid desiccant cycle is the membrane used in the regenerating and dehumidifying section. The dehumidifier and regenerator consist of the liquid desiccant flowing in the permeable polypropylene pipes. The permeable pipes couple the mass and heat transfer between the liquid desiccant and the surrounding air. Temperature and concentration of the desiccant solution exiting the permeable pipes must be calculated by the model for the given inlet desiccant flow temperature and concentration. In this work, the validated

model of Keniar, Ghali, and Ghaddar (2015) is used where they solved for the temperature and concentration changes inside the permeable pipe by applying conservation laws of mass and energy on the desiccant solution. The equations were derived under the following assumptions: 1-D moisture and heat variation; no mass or energy storage in the pipe membrane (quasi-equilibrium model); the liquid desiccant solution is ideal; and the axial vapour diffusion and heat conduction in the pipe are neglected. With these assumptions, the energy equation for the desiccant solution was given by Keniar, Ghali, and Ghaddar (2015) as follows:

$$h_{fg}\rho_a U_m (w_a - w_d) - \dot{m}_d \frac{d}{dy} [h_d(1+c)] + U_c(T_a - T_d) = 0, \quad (1)$$

where U_m and U_c represent the overall mass and heat transfer coefficients per unit length, w_a is the humidity ratio of the surrounding air, w_d is the equilibrium humidity of the desiccant solution, T_d is the desiccant temperature, \dot{m}_d is the desiccant flow rate, and c represents the concentration of water per dry basis. The species conservation equation of the permeable pipes was given by Keniar, Ghali, and Ghaddar (2015)

$$\rho_a U_m (w_a - w_d) - \dot{m}_d \frac{dc}{dy} = 0. \quad (2)$$

The first term represents the vapour transfer from the surrounding air to the desiccant solution and the second term represents the net moisture convective flow. In the experimental validation of Keniar et al.'s (2015) work, forced laminar air conditions were used as part of the experimental constraints and the average calculated convection coefficient was 3.1 W/m K, which is close to the case of natural convection. In the previous case study of Keniar, Ghali, and Ghaddar (2015), the membrane piping system was vertically installed on one of the room walls where natural convective conditions prevailed, while in the current study the piping system is assumed horizontal and natural convection conditions apply. The calculation of the external convection coefficient of the pipes was carried out similar to that in other studies (Eldeeb, Fauchoux, and Simonson 2013; Vashistha and Talukdar 2013).

3.2. DV space model

For the DV system, a chiller provides the cold water required to reduce the supply air temperature passing through the cooling coil. In DV, the supply fresh cool air enters the room at the floor level and displaces the warmer air that rises due to buoyancy effect to reach the ceiling level where they are exhausted (Yuan, Chen, and Glicksman 2001).

The office space considered in this study is modelled in order to assess the comfort level of the occupants in the space. The space is divided into two different zones:

a thermally comfortable zone with an acceptable air quality and an upper contaminated zone where neither thermal nor IAQ is of a concern. The temperature and humidity are found in each zone as well as the temperature gradient and stratification height. The two different zones are separated by the stratification height formed due to air buoyancy effects inside the room induced by the internal load elements. The stratification height is the level at which the flow in the plumes becomes equal to the supply flow rate separating the space into the two zones: occupied and contaminated zones (Novoselac and Serbric 2002). To calculate the stratification height, the upward air flow rate due to the plumes is determined. Assuming that the walls are at uniform inner surface temperature calculated generally from wall 1-D model of transient conduction from the environment to indoor wall, the volumetric flow rate of the upward flow (plume) is given by Mundt (1996) as follows:

$$Q_u = 2.8 \times 10^{-3} |\Delta T|^{2/5} z^{6/5} l, \quad (3)$$

where ΔT is the temperature difference between the wall and lumped indoor air, z is the height of the wall, and l is the horizontal width of the wall.

The plume generated from a point heat source with a heat transfer rate q can be determined by solving Equations (4a)–(4c) for a zone with internal air having a temperature gradient (Mundt 1996) and is expressed as follows:

$$Q_{\text{plume}} = 0.00238 \times q^{3/4} \left(\frac{dT_a}{dz} \right)^{-5/8} \times B_1, \quad (4a)$$

$$B_1 = 0.004 + 0.039A_1 + 0.38A_1^2 - 0.062A_1^3, \quad (4b)$$

$$A_1 = 2.86 \times Z \left(\frac{dT_a}{dz} \right)^{3/8} q^{-1/4}. \quad (4c)$$

Thus, the equation used to determine the stratification height is given by

$$Q_s = NQ_{\text{plume}} + \sum_{k=1}^n Q_{u,k}, \quad (5)$$

where Q_s is the supply air volumetric flow rate, N is the number of point sources inside the room, and n is the number of walls.

The sensible energy balance for the lower occupied zone may be written after applying the first law of thermodynamics as follows:

$$m_{a,1} C_{p,a} \frac{dT_{a,1}}{dt} = \sum_{j=1}^j h_i A_{w,i} (T_w - T_{a,1}) - \dot{m}_s C_{p,a} (T_{a,1} - T_s) + q_{\text{elec}} + q_{\text{people}}. \quad (6)$$

For the upper contaminated zone, the sensible energy balance may be written as

$$m_{a,2} C_{p,a} \frac{dT_{a,2}}{dt} = \sum_{j=1}^j h_i A_{w,i} (T_w - T_{a,2}) - \dot{m}_s C_{p,a} (T_{a,2} - T_{a,1}) - \sum_{i=1}^n \int_0^l U_c (T_{a,2} - T_{d,i}) dy + q_{\text{light}}. \quad (7)$$

In Equations (6) and (7), $A_{w,i}$ is the wall area in each zone, m_a is the air mass for the corresponding zone, h_i is the internal convective heat transfer coefficient, \dot{m}_s is the supply air mass flow rate, T_a is the air temperature for the corresponding zone, and $T_{d,i}$ is the desiccant temperature at element i of the pipe. Note that the wall temperature is obtained from the transient 1-D conduction model through the wall thickness, and the inner wall surface boundary condition includes heat exchange with adjacent room air in each air layer and radiative exchange with the CC (Ayoub, Ghaddar, and Ghali 2006).

Unlike the previous study done on CC/DV systems (Mossolly et al. 2008; Keblawi et al. 2009), the humidity in this study was calculated in each zone separately, since the supply humid air enters the room at the lower zone and rises while carrying more humidity from the occupied zone and ensuring no condensation on the ceiling before it exists at the ceiling level. The mass balance equation for the lower occupied zone is given by

$$m_{a,1} \frac{dw_{a,1}}{dt} = \dot{m}_s (w_s - w_{a,1}) + \frac{Q_{\text{latent}}}{h_{fg}}. \quad (8)$$

For the upper recirculation zone, the mass balance is written as

$$m_{a,2} \frac{dw_{a,2}}{dt} = \dot{m}_s (w_{a,1} - w_{a,2}) - \sum_{i=1}^n \times \int_0^l U_m \rho_a (w_{a,1} - w_{d,i}) dy, \quad (9)$$

where w_s is the supply air humidity ratio, w_a is the internal room air humidity ratio, and $w_{d,i}$ is the liquid desiccant humidity ratio at element i of the indoor pipe with length l .

Since the chilled membrane ceiling system has no direct influence on the humidity conditions of the occupied zone, the occupants could be exposed to higher humidity conditions that could affect their overall thermal comfort. For this reason, the assessment of the overall comfort is necessary using both the ASHRAE (2013), where dT_a/dz should be less than $2.5^\circ\text{C}/\text{m}$ and the Predicted Mean Vote (PMV) is between $+0.5$ and -0.5 on the comfort scale of Fanger (1982) from -3 to $+3$. Since the proposed system does not control humidity within the space, the PMV constraint is included to ensure that thermal comfort conditions are attained through control of the system design

variables of desiccant temperature, supply flow rate, and supply air temperature. In addition, the driving potential for mass moisture transport, the difference between the humidity ratio of the surrounding air, w_a , and the equilibrium humidity of the desiccant solution, w_d , should always be positive.

3.3. Modelling of solar collectors

In order to decrease the operational cost of the system, solar irradiance is used as an energy source to supply the required heat for the regeneration of the liquid desiccant. A parabolic solar collector is used because it occupies less space and is very efficient compared to other types of solar heating systems. The performance of the collector-tank system is simulated using the theory of Hottel and Whillier presented by Duffie and Beckman (2003) to estimate the heat gain by water flowing in the solar collector and the transient water temperature in the water storage tank, which will be modelled as well-mixed represented by one uniform temperature.

3.4. LDMC-C/DV integrated simulation model and its validity

The component models are coupled with the space model. The LDMC-C/DV system simulation model needs the following inputs: the space dimensions, wall properties, ambient conditions, dimensions of the permeable pipes, and physical properties of the desiccant. The wall model is solved using an explicit finite difference scheme, with convergence satisfied for a simulation time step of 60 seconds and a wall increment of 100 divisions perpendicular to the wall surface and along the wall thickness where highest gradients of temperatures exist from outside to inside, and the inner wall temperature and the average heat gained by the wall are calculated for every hour. The pipes of the dehumidifier and regenerator are discretized into 100 elements in order to account for the concentration and temperature variation along the length of the pipe. The solar system is simulated for a period of 12 h, by taking the needed regeneration energy along with the hourly solar flux as inputs. A simulation code program, using MATLAB[®] (Mathworks 2015), is developed based on the discrete form of systems and space model equations with imposed boundary and initial conditions. The choice of MATLAB[®] computing environment is made to facilitate the interaction between the model simulation results and the use of the optimization tool; the genetic algorithm procedure on MATLAB[®] when considering the LDMC-C/DV optimization be described in Section 4.

The model assumed initial wall temperatures in order to compute the energy gained by the multilayer walls of the space model. The dehumidifier model computes the amount of sensible and latent load removed by the membrane system. After that the space model computes the

room temperature and updates the internal wall temperature that takes into consideration the radiative energy exchange with the cool ceiling. The iterative procedure is repeated until convergence is reached. Convergence is considered to be reached if the difference in the norm of the wall temperatures between two iterations is less than 0.01 K. After calculating the internal wall temperatures, the space model computes the stratification height and the space is then divided into two zones and the temperature and humidity are calculated at every zone. The regenerator model is used to calculate the regeneration temperature and the temperature at the exit of the regenerator. Knowing the inlet and exit temperatures at the dehumidifier and regenerator, the cooling and heating energies of the desiccant cycle are evaluated. The well-mixed storage tank model integrated to the solar collector estimates the storage tank temperature at each hour; if this temperature is not sufficient to cover the thermal energy needed, auxiliary energy is used.

All the component models considered in this work, mainly the DV system coupled with CC and the model of desiccant membrane integrated with the solar system, were validated extensively in the literature (Ayoub, Ghaddar, and Ghali 2007; Mossolli et al. 2008; Keblawi et al. 2009; Keniar, Ghali, and Ghaddar 2015). The simulation model results will be used in the optimization methodology that assesses the performance of the system under colder CC conditions and warmer DV supply flow rates not considered in conventional CC/DV operational ranges to determine the optimal settings for the given space load and ambient conditions.

4. Optimization methodology

Modelling the liquid desiccant system with the LDMC-C/DV system is a complex task with multivariables involved and coupled equations with indirect relations existing between different parameters. Since several non-linear equations are solved, a revolutionary derivative-free optimization tool was used following the direct search technique (House and Smith 1995). The simplest optimization tool that could be used for the proposed case is the genetic algorithm optimization tool because it is derivative free and is somehow efficient if compared with other derivative-based optimization schemes (Niu, Zhang, and Zuo 2002; Mossolli, Ghali, and Ghaddar 2009; Keblawi, Ghaddar, and Ghali 2011). Moreover, it fetches the global minimum of a specific function.

For the optimized control strategy used for the LDMC-C/DV system and by referring to Figure 1, the variables that are used for cost optimization are the desiccant temperature at the inlet of the dehumidification membrane (T_1), the supply air temperature (T_s), and the supply air mass flow rate (\dot{m}_s). Each variable in the optimization routine has a lower and an upper bound that defines the interval where the genetic algorithm searches for the optimal cost

and are based on physical considerations. The bounds for the different variables are as follows:

- The supply air temperature is considered to vary between 17°C and 23°C to reduce draft and ensure thermal comfort (Kebrawi, Ghaddar, and Ghali 2011).
- The supply air mass flow rate is considered to vary between 0.08 and 0.26 kg/s to maintain the stratification height above 1 m (Kebrawi, Ghaddar, and Ghali 2011). The minimum supply flow rate of 0.08 kg/s corresponds to the stratification height of 1 m. Since the supply flow rate is 100% fresh air, it ensures that the occupants are breathing fresh air entrained into their thermal plume from the lower clean zone of the space.
- The temperature of the liquid desiccant entering the dehumidifier ranges between 12°C and 20°C to ensure that dehumidification takes place inside the space.

There are several non-linear constraints that are applicable to the system. These constraints are related to thermal comfort issues and physical constraints. The constraints may be redefined in the following list:

- The temperature gradient does not exceed 2.5°C/m. This condition is required so that the person is not subject to large gradients in temperature between the head and feet that cause thermal discomfort (ASHRAE 2009).
- The PMV in the occupied zone “PMV” is within ± 0.5 for thermal comfort.
- The stratification height inside the room is greater than 1 m. This condition is required so that the stratified air does not mix with the breathing zone (ASHRAE 2009).

To enhance the speed of the genetic algorithm, the electrical cost function and constraints are combined in a single cost function by using penalty functions; thus, the fitness cost function may be written as

$$J = \alpha_{\text{elec}} \times C_{\text{elec}} + \alpha_{\text{tgrad}} \times C_{\text{tgrad}} + \alpha_{\text{stratH}} \times C_{\text{stratH}}. \quad (10)$$

The coefficients α_{elec} , α_{tgrad} , and α_{stratH} in the above function are the weight factors for electrical energy consumption (operational) cost (C_{elec}), temperature gradient cost (C_{tgrad}), and stratification height cost (C_{stratH}), respectively, and are set according to the system parameter. For the current system, the weight factors are set to unity.

The cost of the chiller is calculated by using the following equation:

$$E_{\text{chiller}} = \frac{Q_{\text{cooling}}}{1000 \times \text{COP}_{\text{chiller}}} = \frac{Q_d + Q_s}{1000 \times \text{COP}_{\text{chiller}}}, \quad (11)$$

where Q_d is the cooling energy needed for liquid desiccant, Q_s is the cooling energy needed for the supply air, and $\text{COP}_{\text{chiller}}$ is the coefficient of performance of the chiller assumed to have an average value of 3.5. The cooling energy needed for the supply air in kW is given by

$$Q_s = \dot{m}_s(h_a - h_s), \quad (12)$$

where \dot{m}_s is the supply air mass flow rate, h_s is the enthalpy of supply air, and h_a is the enthalpy of the outdoor air. The cooling energy needed for liquid desiccant in kW is given by

$$Q_d = \dot{m}_d(h_{d,7} - h_{d,1}), \quad (13)$$

where \dot{m}_d is the liquid desiccant mass flow rate and h_d is the enthalpy of liquid desiccant at points 1 and 7 (refer to Figure 1). Note that the ceiling panel is removing some latent load to prevent condensation, while in the conventional CC/DV system, the DV system removes the latent load before entering the room using a sub-cooling technique and thus, a higher relative humidity (RH) is expected in the space, but condensation on the ceiling is prevented. The DV supply air dew point temperature is lowered below the ceiling temperature in the conventional CC/DV. In addition, spaces conditioned by the conventional CC/DV system are characterized by a humidity that is almost uniform in the whole space (lower occupied zone and upper recirculation zone). However, in the membrane system, there are two zones of humidity: a lower zone of higher humidity and an upper zone of lower humidity, where dehumidification occurs at the ceiling with minimal mixing between the two zones because of the natural upward motion of the air. The higher humidity in the occupied zone with the membrane system will affect the perceived air quality as described in Fang, Clausen, and Fanger (1998a, 1998b) and Simonson, Salonvaara, and Ojanen (2002), and may also affect many other parameters such as durability of the building materials (Fang et al. 2004).

The fan cost is directly related to the air mass flow rate by using the following equation (House and Smith 1995):

$$E_{\text{fan}} = \left(\frac{200}{3600} \right) \left(\frac{\dot{m}_s^3}{1.29} \right), \quad (14)$$

where \dot{m}_s is the supply air mass flow rate. The auxiliary energy needed in case the solar energy is not sufficient is calculated as follows:

$$E_{\text{aux}} = \dot{m}_d(h_{d,5} - h_{d,4}), \quad (15)$$

where \dot{m}_d is the liquid desiccant mass flow rate and h_d is the enthalpy of the liquid desiccant at points 4 and 5 (see Figure 1). Therefore, the total energy consumed can be expressed by the following equation:

$$C_{\text{elec}} = E_{\text{fan}} + E_{\text{chiller}} + E_{\text{aux}}. \quad (16)$$

In the above equation, the auxiliary heater is assumed to be an electric heater at 100% efficiency. The electric heater

is selected since it is the common practice in Lebanon where there are no gas distribution lines to supply gas to buildings. In addition, the solar energy system has been sized to minimize auxiliary heat use. The different cost functions defined above are expressed as follows (Niu, Zhang, and Zuo 2002; Mossolly, Ghali, and Ghaddar 2009; Keblawi, Ghaddar, and Ghali 2011):

$$C_{\text{stratH}} = \exp\left(\frac{H_{\text{min}}}{H}\right) - 1, \quad (17a)$$

$$C_{\text{tgrad}} = \exp\left(\frac{dT/dz}{(dT/dz)_{\text{max}}}\right) - 1. \quad (17b)$$

The exponential term helps to restrict the cost function variables between their upper and lower bound limit. If the value of each variable exceeds the upper bound, the value of the cost function will increase dramatically and the set of variables will be rejected. The use of exponential form to control the constraints' cost and the integration of the constraint terms within the objective function expression were implemented by Keblawi, Ghaddar, and Ghali (2011) and Hammoud, Ghali, and Ghaddar (2014).

5. System optimization solution methodology

In order to optimize the operation of the LDMC-C/DV system, the optimizer will generate random values of the controllable variables and use these values in the system MATLAB[®] simulation model to predict the room temperature gradient, stratification height, and other needed parameters for the evaluation of the cost function (see Equation (10)) and the constraints of thermal comfort and air quality. The optimizer model uses genetic algorithm procedures implemented on MATLAB[®] and checks for the constraints and calculates the cost function for the selected set of variables. The interaction between the model simulation and the optimization tool (genetic algorithm) is a continuous process until finding the optimal values of the controllable variables with minimum cost function for each prediction period of 1 h. The optimization tool searches for the optimum values of the set points for every prediction period. The genetic algorithm maximum population size is chosen to be 60 with a 0.6 crossover value, 10^{-3} tolerance function, and a stall time limit of 150. The weight factors for electrical cost, temperature gradient cost, and stratification height cost are set to be unity. The flow chart shown in Figure 2 describes the path followed to obtain the optimal set points for the proposed combined system. The simulation of the system is performed for each hour over the 12 h of system operation.

Optimization is done for different operational strategies. A two-variable optimized strategy is performed at a fixed liquid desiccant temperature, while varying the DV supply air temperature and flow rate to study the effect of lowering the ceiling temperature on system performance.

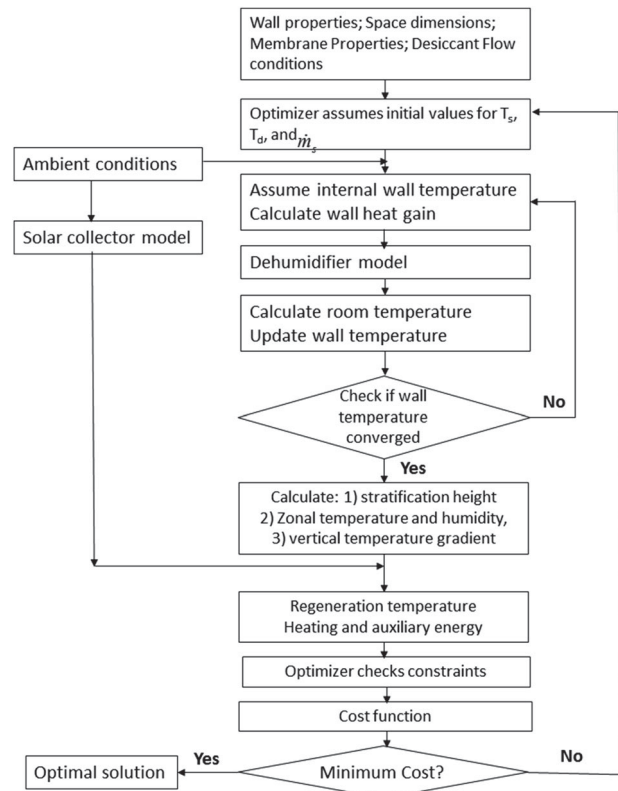


Figure 2. Flow chart of system optimization methodology.

This is achieved by considering two different liquid desiccant inlet temperatures such that one resulting ceiling temperature would be close to values obtained in the conventional CC/DV, while the other is significantly lower than the conventional range. This is followed by optimizing the system operation by a three-variable control strategy comparing its performance with the conventional CC/DV system.

6. Description of the case study

In this work, the case study of Keblawi, Ghaddar, and Ghali (2011) is used with the same space properties and same ambient conditions. Their case study was for a typical office in Beirut of dimensions $5\text{ m} \times 5\text{ m} \times 3\text{ m}$ with floor area of 25 m^2 . The office consisted of four walls, two external at the south and the west direction, where the east and the north ones were considered partitions. Each wall was composed of three layers of typical Lebanese building construction with properties provided in Table 1. Figure 3 illustrates the sensible and latent load schedules inside the office. The maximum number of space occupants is 6 and the space is occupied from 7 am till 6 pm. The maximum latent load due to external and internal generation from occupants is 410 W. The total internal and external sensible load that the system should remove reaches a peak of

Table 1. Wall layer properties.

Layer number	Layer material	Thickness (mm)	Density (kg/m ³)	Specific heat (kJ/kg K)	Thermal conductivity	R-value (m ² K/W)
1	Gypsum Board	15.8	800.9	1.09	0.161	0.09862
2	LW Concrete Block	101.6	608.7	0.84	0.38	0.26681
3	Face Brick	101.6	2002.3	0.92	1.33	0.07626

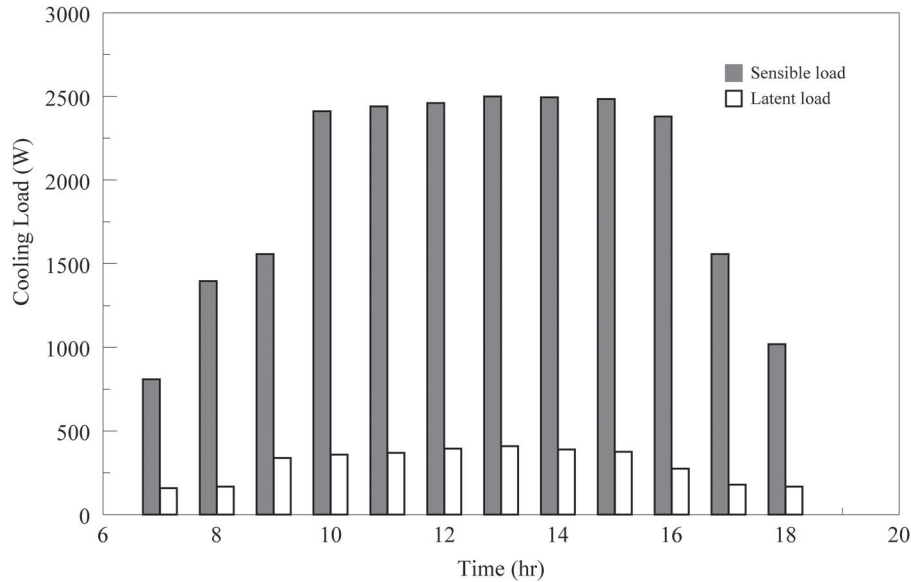


Figure 3. The hourly variation of the internal sensible and latent loads of the office space.

99 W/m², which is higher than the ability of the DV system.

The liquid desiccant pipes are assumed to be made of polypropylene. The length of each pipe was equal to the ceiling length, which is 5 m, and the number of pipes was 120 each with a diameter of 2.3 cm and thickness of 0.2 mm. The membrane material properties were taken as 5.2×10^{-7} m²/s for material vapour diffusivity and 0.34 W/m K for thermal conductivity.

For the liquid desiccant entering the pipes inside the room, the desiccant concentration was set to a fixed value of 38%, which achieves dehumidification at desiccant temperature lower than 20°C without the risk of crystallization (Elsayed, Gari, and Radhwan 1992). The desiccant mass flow rate was chosen to be 3.6 kg/h per pipe (Keniar, Ghali, and Ghaddar 2015) in order to cover the whole pipe area and to ensure that enough heat and moisture were transferred to the pipes. The properties of the regeneration tubes (diameter and number) were the same as that of the dehumidification pipes; but at length of 1 m to prevent the decrease in the desiccant temperature during interaction with the ambient air because of the large difference between the regeneration temperature and the ambient temperature and the low desiccant flow rate inside the tubes. The regeneration temperature was varied to

provide the 38% desiccant concentration at the inlet of the dehumidifier. The optimization model was performed for a typical day in August with ambient conditions shown in Table 2.

After calculating the thermal energy required for the regeneration of the liquid desiccant, the storage tank and the parabolic solar panels were sized. A total of 4.8 m ×

Table 2. Ambient conditions for the month of August (Ghaddar and Bsai 1998).

Hour	Ambient temperature °C	Ambient humidity ratio kg _w /kg _a	Horizontal surface solar flux W/m ²
7:00	24.6	0.0177	343.9
8:00	25.8	0.0177	504.7
9:00	27.3	0.0176	646.2
10:00	28.8	0.0177	746.3
11:00	29.9	0.0178	769.3
12:00	30.7	0.0177	790.6
13:00	31.3	0.0178	688.8
14:00	31.6	0.0177	559.6
15:00	31.6	0.0177	403.1
16:00	31	0.0178	241.3
17:00	30.1	0.0177	193.5
18:00	29.1	0.0177	94

1.2 m parabolic collectors and a storage tank with 1 m³ can supply the system with the required thermal energy. The solar concentrators and storage tank were selected to occupy not more than 25% of the roof area. The specifications of a single parabolic collector were presented by Audah, Ghaddar, and Ghali (2011).

7. Results and discussion

7.1. Effect of varying liquid desiccant temperature on LDMC-C/DV on energy performance

Optimization is performed for two cases A and B each at a fixed liquid desiccant temperature with two operational variables to be optimized (supply temperature and flow rate). In the first case (case A), the desiccant temperature is fixed at 16°C, while in case B the desiccant temperature is set to 13°C. Table 3 presents all operational set points for cases A and B.

For case A, the DV supply temperature of the air was highest and the air flow rate was lowest in the early morning, since the loads inside the space were low at this period (see Figure 3). As the space load increased, the DV supply air temperature decreased to reach minimum values of 18.03°C at the mid of the day, while the supply air mass flow rate increased to maximum values of 0.221 kg/s. The ceiling temperature was lower for case B, resulting in higher DV supply temperature and lower DV supply flow rate to maintain the indoor comfort conditions. For case B, the variation in the supply temperature, ceiling temperature, and mass flow rate had similar trends to that in case A.

Figure 4 shows the needed cooling energy of DV supply air and the liquid desiccant flow and the needed heating regeneration energy for cases A and B. The total cooling energy and the heating energy for the LDMC-C/DV system increase as loads in the space and ambient temperature increase for both cases A and B. The DV cooling energy

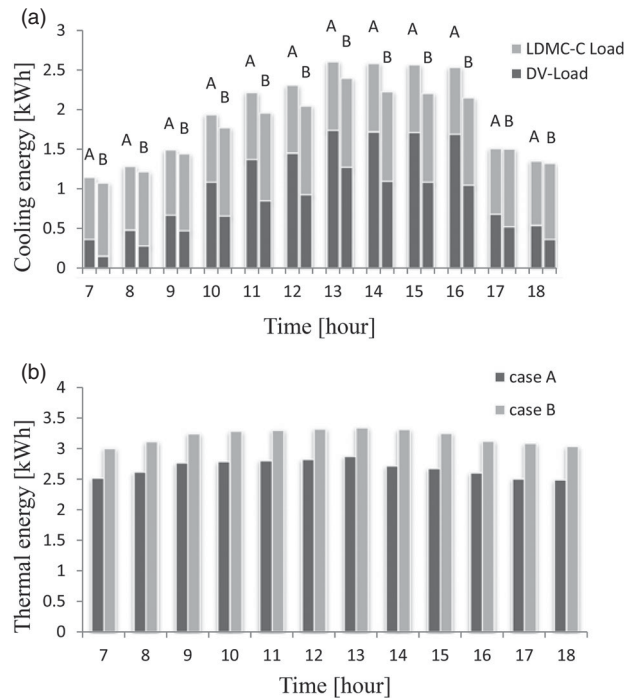


Figure 4. Plots of (a) cooling energy and (b) thermal energy for regeneration needed for both cases A and B.

was less for case B, because of the higher supply temperatures and lower mass flow rates. The desiccant cooling energy in case B is higher than that of case A, while the DV cooling energy is lower in case B than that required in case A. However, the total cooling energy in case B is less than that of case A by 10%. As a result, the heating regeneration energy needed for desiccant regeneration in case B is more than the heating regeneration energy needed in case A. This means a smaller size chiller would be needed in case B than that of case A while meeting both constraints of PMV and air quality.

Table 3. Hourly optimized set points for supply air temperature and supply air flow rate, and the ceiling temperature for cases A and B.

Hour	Case (A) desiccant temperature 16°C			Case (B) desiccant temperature 13°C		
	T _s (°C)	T _c (°C)	Supply air mass flow rate (kg/s)	T _s (°C)	T _c (°C)	Supply air mass flow rate (kg/s)
7	20.19	17.77	0.086	22.28	15.50	0.083
8	19.41	18.01	0.114	21.90	16.00	0.099
9	19.36	18.21	0.137	20.90	16.20	0.119
10	18.44	18.46	0.178	20.41	16.72	0.151
11	18.18	18.50	0.200	20.31	16.79	0.175
12	18.18	18.51	0.204	20.47	16.80	0.186
13	18.03	18.53	0.221	19.27	16.83	0.198
14	18.04	18.49	0.219	19.38	16.79	0.186
15	18.09	18.43	0.214	19.44	16.73	0.166
16	18.23	18.41	0.208	20.10	16.68	0.164
17	19.33	18.29	0.092	21.07	16.38	0.085
18	19.47	17.80	0.087	21.52	15.66	0.082

7.2. Optimized LDMC-C/DV operation and performance comparison with conventional CC/DV

The consideration of lower CC temperatures in cases A and B has resulted in a lower cooling load. In this section, the optimization is presented on case C where the three operational parameters (supply temperature, desiccant temperature, and flow rate) are set to be variable. Energy performance comparison is made with the conventional CC/DV operating with the same operational conditions.

For case C of optimized operation in which the three variables change (see Table 4), the supply air temperature varied between 21.24°C and 19.83°C, the liquid desiccant temperature between 18.12°C and 12.57°C, and the supply air mass flow rate between 0.091 and 0.186 kg/s. When both sensible and latent loads reached their peaks at mid-day at 2500 and 410 W, respectively, the optimizer increased the supply flow rate and decreased the supply air temperature and the desiccant temperature, allowing the system to remove the higher load from the space. As a result, the cooling energy for the DV system and liquid desiccant and the heating energy needed for desiccant regeneration increased. During the whole operation hours of the system, the available solar energy was sufficient to regenerate the liquid desiccant; therefore, no auxiliary heating energy was used.

Figure 5 shows the variation with time of (a) the vertical temperature gradient dT/dz , (b) the stratification height, and (c) the PMV for case C. The temperature gradient dT/dz was less than 2.5°C/m, which means that thermal comfort is maintained in the office (ASHRAE 2013), but the occupants could be exposed to higher humidity conditions in the presence of membrane CC that could affect their overall thermal comfort; but the value of the PMV in the occupied zone was found to be less than 0.3, which is

Table 4. Hourly optimized set points of the LDMC-C/DV system for supply air temperature and supply air flow rate, and the desiccant temperature (Case C).

Case (C) optimized operation of LDMC-C/DV system where three variables change			
Hour	T_s (°C)	T_d (°C)	Supply air mass flow rate (kg/s)
7	21.24	18.12	0.091
8	21.17	17.23	0.127
9	21.01	16.13	0.139
10	20.83	13.35	0.153
11	20.73	12.72	0.157
12	20.42	12.64	0.176
13	19.83	12.57	0.186
14	19.97	12.61	0.181
15	20.22	13.32	0.175
16	21.24	18.12	0.091
17	21.17	17.23	0.127
18	21.01	16.13	0.139

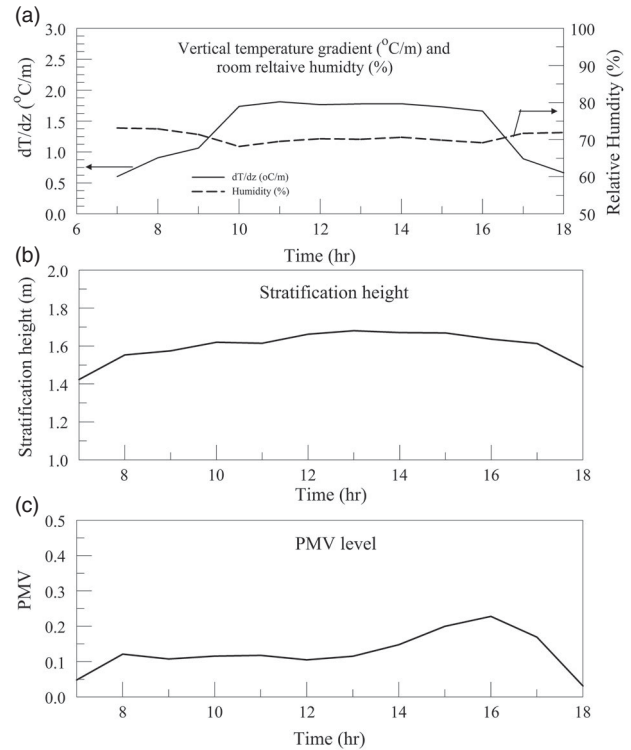


Figure 5. Plots of (a) the room vertical temperature gradient dT/dz and RH (%), (b) the stratification height for case C, and (c) the PMV for case C.

an acceptable level of thermal comfort and meets the set constraint.

In comparing the variation of variables and total energy needed in case C with the previous two cases A and B, it is clear that the optimizer selected a lower desiccant temperature than the previous cases A and B (see Table 3). Moreover, the supply temperature was higher and the supply flow rate was lower for most of the hours in case C. As a result, the total cooling energy in case C is less than that in cases A and B. As a conclusion, implementing the optimization strategy with three variables (supply temperature, desiccant temperature, and supply flow rate) leads to energy saving more than that in the case of optimization with two variables (supply temperature and supply flow rate). It is to be noted that in the three cases (A, B, and C), the occupied zone is below the stratification height and the occupants are basically breathing fresh air of high air quality. Cases B and C might have higher IAQ for a standing person, which is not considered in the current study. The DV systems are considered high air quality systems because it provides fresh air to the occupied zone only, which could represent 1/3 of the height of the space.

The energy comparison between the LDMC-C/DV optimized system and a conventional CC/DV system is performed at the same input conditions. The conventional CC/DV systems have the same supply air temperature, supply air mass flow rate, and average ceiling temperature of the LDMC-C/DV system of case C. However, to

prevent ceiling condensation and to deliver the DV air at the required temperature, the DV supply air was sub-cooled to lower its dew point temperature below the ceiling temperature followed by reheat. This will bring the same air temperature distribution in the two systems but not the same RH. It is higher in the membrane systems, but since human thermal comfort can tolerate a wider range of humidity as compared to temperature, the PMV did satisfy the comfort acceptability constraint within ± 0.5 for both systems. The conventional optimized CC/DV system leads to a comfort level at the cooler side where the PMV varies between -0.48 and -0.2 for the same hours of operation compared to the current system, where it varied between 0.05 and 0.2 . The RH level in the conventional CC/DV system for the same input conditions is also lower than that of the current system due to the CC condensation prevention condition. The minimum and maximum RH values in the space for the conventional CC/DV system were 50.1% and 70.2% , respectively, compared to 68.2% and 73.2% , respectively, in the LDMC-C/DV system of case C (see Figure 5(a)).

The DV cooling energy for the LDMC-C/DV system, as shown in Figure 6, is less than that of a CC/DV conventional system operating with the same conditions, since the latent load and a part of the sensible are removed in the DV section of the conventional system. On the other hand, the CC cooling energy is lower for the conventional system due to the removal of humidity by the liquid desiccant

in the LDMC-C/DV system which requires a regeneration process and more cooling energy. The total cooling energy of the LDMC-C/DV system is less than the total cooling energy of the CC/DV system; as a result, a smaller chiller size is used. The thermal energy needed for desiccant regeneration in the LDMC-C/DV system is higher than the heating energy needed for supply air reheat in the conventional CC/DV systems; however, the solar system is used as a free renewable energy source to make the LDMC-C/DV more efficient. Note that a condenser or a solar energy system could be used as “free” reheat in both membrane and conventional. In the current study, the thermal energy needed for heating and electrical energy for cooling were not added. However, in the economic analysis comparison of the two systems that follows in the next section, electrical energy is assumed for the reheating in the conventional CC/DV system to prevent including the heat exchange cost with the condenser and the variation of its operation.

7.3. Economic analysis

The economic feasibility of the proposed LDMC-C/DV system is compared to a conventional CC/DV system using the same input and operating conditions of case C (Figure 7) and taking into consideration that the comfort level between the two systems may slightly differ but is maintained with the same constraints in both the conventional and proposed membrane systems. The supply air temperature, supply air mass flow rate, and average ceiling temperature of the conventional CC/DV system are chosen to be the same of the optimized values obtained for the LDMC-C/DV system at each hour. The comparison of the energy consumption for the two systems is done for typical days for May, June, July, August, and September. The total monthly energy consumption can be calculated by multiplying the daily total energy by the numbers of days of the month. Higher values of electrical power consumption

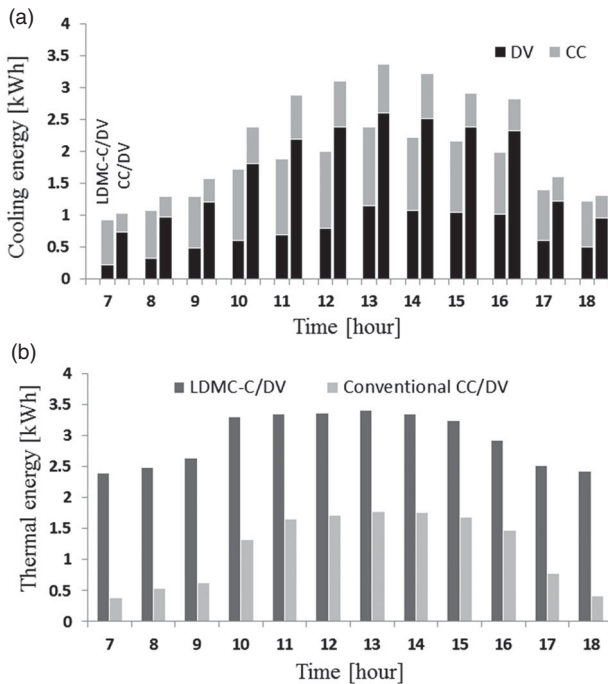


Figure 6. Plots of (a) cooling energy and (b) thermal energy needed for case C of the LDMC-C/DV system with comparison with the conventional CC/DV system.

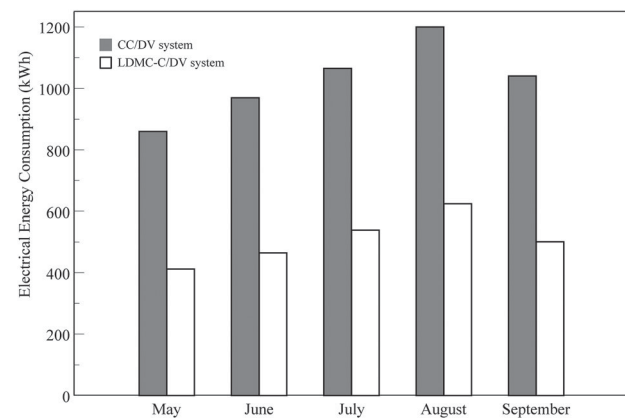


Figure 7. Comparison of energy consumption over cooling season.

are considered in the conventional CC/DV system, due to additional cooling and reheat energy. In the conventional CC/DV system, humidity is removed by reducing the supply air temperature below the ceiling dew point, to prevent water vapour condensation on the ceiling. After reaching the required humidity ratio, the supply air will be reheated electrically to the specified supply temperature.

Figure 7 shows the total electrical energy consumption of the LDMC-C/DV system and the conventional CC/DV system during the five months of the cooling season. The maximum electrical energy consumed as well as maximum energy saving was observed during the month of August due to the high levels of ambient temperature and humidity ratios. By comparing the total energy consumption of the two systems, it is clear that the LDMC-C/DV system consumes 49% less than the conventional CC/DV system. Therefore, by considering the electrical cost of 0.15 \$/kWh in Beirut, the amount of electricity saving over the operational period of 5 months per year is calculated to be about \$390.

The cost of installing the proposed system will be compared to the cost of installing the conventional CC/DV system in addition to the cost of electricity consumed every year, in order to determine the payback period. The cost of the proposed system includes the initial costs of the dehumidification/regeneration pipes and the parabolic solar panels. The length of parabolic collectors required to supply the thermal energy for desiccant regeneration is 4.8 m with a 1.2 m width. The estimated cost of the solar collectors is \$2000 (Audah, Ghaddar, and Ghali 2011). As for the membrane, the material used costs 5 \$/m² (Larson 2006), which implies a total material cost of \$220. The cost of installation and fabrication of the membrane pipes is estimated as \$500 (Keniar, Ghali, and Ghaddar 2015). The maintenance cost of the system was added at 10% of the initial cost annually. Therefore, the total cost of the proposed system is \$2720. On the other hand, the cost of installing CC panels is taken to be 36 \$/m², so the initial cost of the panels is \$900. The additional cooling required by the CC/DV system is estimated to be 5 kW, resulting with \$500 as the incremental initial chiller cost. The initial cost of using the proposed system is thus \$1320 more than that of the CC/DV system. In order to determine the present worth value of both the systems, Equations (19a) and (19b) are used.

$$P = A_0 \frac{1 - ((1 + i)/(1 + d))^n}{d - i}, \quad i \neq d, \quad (18a)$$

$$P = A_0 \frac{n}{1 + d}, \quad i = d. \quad (18b)$$

In Equations (18a) and (18b), P represents the present worth, n is the number of years, d is the discount rate, and i is the annual rate at which electricity costs are increasing. Using a discount rate of 2% and an annual rate of electricity price increase as 3%, the payback period is calculated

to be four years and three months when implementing the proposed LDMC-C/DV system in this study.

8. Conclusions

In this study, a dehumidification membrane system has been used as a cooled ceiling panel and was combined with DV system to operate inside a typical office in Beirut city. The LDMC-C/DV system prevents condensation on the ceiling and hence permits the use of lower CC temperatures that are normally constrained in conventional CC/DV systems. The performance of the proposed system was studied using integrated models of the system components and space plus walls models. Optimized operational strategies based on genetic algorithm were also used to predict the optimal set points (CC temperature, supply air temperature, and flow rate) of the combined system using two- and three-variable strategies. Based on the simulations of the system for three cases, the following is concluded:

Decreasing the desiccant ceiling temperature resulted in higher cooling energy for cooling the ceiling and lower DV cooling energy because of the higher supply temperatures and lower mass flow rates. However, the total cooling energy required from the chiller decreased by 10% with a decrease in the desiccant ceiling temperature by 3°C, although the regeneration thermal energy increased.

Implementing the optimization strategy with three variables (supply temperature, desiccant temperature, and supply flow rate) leads to energy saving more than the case of optimization with two variables (supply temperature and supply flow rate).

The energy analysis of the combined system showed that 49% energy saving was achieved compared to the conventional CC/DV system with the same input operational parameters.

The LDMC-C/DV system and the conventional CC/DV system have the same constraint for maintaining thermal comfort as measured by the PMV at ± 0.5 , but their operative parameters may result in slightly different comfort levels as well as humidity level. The conventional optimized CC/DV system leads in the case study to a comfort level at the cooler side where the PMV varies between -0.48 and -0.2 compared the LDMC-C/DV system wherein it varied between 0.05 and 0.2. The minimum and maximum RH values in the space for the conventional CC/DV system were 50.1% and 70.2%, respectively, compared to 68.2% and 73.2%, respectively, in the LDMC-C/DV system for the case of optimized operation with three variables.

The economic analysis showed that the payback period for installing the LDMC-C/DV system is less than five years.

Funding

The authors would like to thank the Lebanese National Council for Scientific Research (CNRS) and the Munib and Angela Masri

Institute for Energy and Natural Resources for their financial support.

References

- Abdel-Salam, A. H., G. Ge, and C. J. Simonson. 2014. "Thermo-economic Performance of a Solar Membrane Liquid Desiccant Air Conditioning System." *Solar Energy* 102: 56–73.
- Abdel-Salam, A. H., C. Mcnevin, L. Crofoot, S. J. Harrison, and C. J. Simonson. 2016. "A Field Study of a Solar Liquid Desiccant air Conditioning System: Quasi-Steady and Transient Performance." *ASME Journal of Solar Energy Engineering* 138 (3): 031009-1150–031009-14. Paper No: SOL-15-1202 (14 pages)
- Abdel-Salam, A. H., and C. J. Simonson. 2016. "State-of-the-art in Liquid Desiccant air Conditioning Equipment and Systems." *Sustainable Energy Reviews* 58: 1152–1183.
- ASHRAE. 2009. *Handbook of Fundamentals. American Society of Heating Refrigerating and Air-Conditioning Engineers*. Chapter 9. Atlanta, GA: American Society of Heating Refrigerating and Air-Conditioning Engineers.
- ASHRAE. 2013. *ANSI/ASHRAE Standard 55-2013: Thermal Environmental Conditions for Human Occupancy. American Society of Heating, Refrigeration, and Air Conditioning Engineers*. Atlanta, GA: American Society of Heating, Refrigeration, and Air Conditioning Engineers.
- Audah, N., N. Ghaddar, and K. Ghali. 2011. "Optimized Solar-powered Liquid Desiccant System to Supply Building Fresh Water and Cooling Needs." *Applied Energy* 88: 3726–3736.
- Ayoub, M., N. Ghaddar, and K. Ghali. 2006. "Simplified Thermal Model of Spaces Cooled with Combined Positive Displacement Ventilation and Chilled Ceiling System." *HVAC&R Research* 12: 1005–1030.
- Ayoub, M., N. Ghaddar, and K. Ghali. 2007. "Chilled Ceiling and Displacement Ventilation System: An Opportunity for Energy Saving in Beirut." *International Journal of Energy Research* 31: 743–759.
- Bahman, A., L. Rosario, and M. M. Rahman. 2012. "Analysis of Energy Savings in a Supermarket Refrigeration /HVA C System." *Applied Energy* 98: 11–21.
- Behne, M. 1999. "Indoor Air Quality in Rooms with Cooled Ceilings: Mixing Ventilation or Rather Displacement Ventilation?" *Energy and Buildings* 30 (2): 155–166.
- Cheng, Q., and X. Zhang. 2013. "Review of Solar Regeneration Methods for Liquid Desiccant Air-Conditioning System." *Energy and Buildings* 67: 426–433.
- Crofoot, L., and S. Harrison. 2012. "Performance Evaluation of a Liquid Desiccant Solar Air Conditioning System." In 1st International Conference on Solar Heating and Cooling for Buildings and Industry (SHC 2012). *Energy Procedia* 30: 542–550.
- Duffie, J., and W. A. Beckman. 2003. *Solar Engineering and of Thermal Processes*. New York, NY: John Wiley & Sons.
- Eldeeb, R., M. Fauchoux, and C. Simonson. 2013. "Applicability of a Heat and Moisture Transfer Panel (HAMP) for Maintaining Space Relative Humidity in an Office Building Using TRNSYS." *Energy and Buildings* 66: 338–345.
- Elsayed, M., H. Gari, and A. Radhwan. 1992. "Effectiveness of Heat and Mass Transfer in Packed Beds of Liquid Desiccant System." *Renewable energy* 3: 661–668.
- Fang, L., G. Clausen, and P. O. Fanger. 1998a. "Impact of Temperature and Humidity on the Perception of Indoor Air Quality." *Indoor Air* 8: 80–90.
- Fang, L., G. Clausen, and P. O. Fanger. 1998b. "Impact of Temperature and Humidity on Perception of Indoor Air Quality During Immediate and Longer Whole-Body Exposures." *Indoor Air* 8: 276–284.
- Fang, L., D. P. Wyon, G. Clausen, and P. O. Fanger. 2004. "Impact of Indoor Air Temperature and Humidity in an Office on Perceived air Quality, SBS Symptoms and Performance." *Indoor Air* 14 (suppl. 7): 74–81.
- Fanger, B. O. 1982. *Thermal Comfort Analysis and Applications in Engineering*. New York: McGraw Hill.
- Fauchoux, M., M. Bansal, C. Simonson, and D. Torvi. 2010. "Testing and Modelling of a Novel Ceiling Panel for Maintaining Space Relative Humidity by Moisture Transfer." *International Journal of Heat and Mass Transfer* 53: 3961–3968.
- Fauchoux, M., C. Simonson, and D. Torvi. 2008. "Investigation of a Novel Ceiling Panel for Heat and Moisture Control in Buildings." In *Proceedings of the 8th Symposium on Building Physics in the Nordic Countries, Danish Society of Engineers*, edited by C. Rode, 1269–1276. Copenhagen, Denmark: Danish Society of Engineers.
- Fauchoux, M., C. Simonson, and D. Torvi. 2009. "Tests of a Novel Ceiling Panel for Maintaining Space Relative Humidity by Moisture Transfer From an Aqueous Salt Solution." *Journal of ASTM International* 6 (4): 1–10.
- Ge, G., A. H. Abdel-Salam, R. W. Besant, and C. J. Simonson. 2013. "Research and Applications of Liquid-to-air Membrane Energy Exchangers in Building HVAC Systems at University of Saskatchewan: A Review." *Sustainable Energy Reviews* 26: 464–479.
- Ge, G., M. Fauchoux, R. W. Besant, and C. J. Simonson. 2014. "State-of-the-art in Liquid-to-Air Membrane Energy Exchangers (LAMEEs): A Comprehensive Review." *Sustainable Energy Reviews* 39: 700–728.
- Ghaddar, N., and A. Bsat. 1998. "Energy Conservation of Residential Buildings in Beirut." *International Journal of Energy Research* 32 (2): 523–546.
- Hammoud, M., K. Ghali, and N. Ghaddar. 2014. "The Optimized Operation of a Solar Hybrid Desiccant/Displacement Ventilation Combined with a Personalized Evaporative Cooler." *International Journal of Green Energy* 11 (2): 141–160.
- Hao, X., G. Zhang, Y. Chen, S. Zou, and D. Moschandreas. 2007. "A Combined System of Chilled Ceiling, Displacement Ventilation and Desiccant Dehumidification." *Building and Environment* 42: 3298–3308.
- House, J., and T. Smith. 1995. "A System Approach to Optimal Control for HVAC and Building Systems." *ASHRAE Transactions* 101 (2): 647–660.
- Jiang, Z., Q. Chen, and A. Moser. 1992. "Indoor Airflow with Cooling Panel and Radiative/Convective Heat Source." *ASHRAE Transactions* 98 (1): 33–42.
- Joege, F., and C. Armando. 2002. "Thermal Behavior of Closed Wet Cooling Towers for Use with Chilled Ceilings." *Applied Thermal Engineering* 20: 1225–1236.
- Keblawi, A., N. Ghaddar, and K. Ghali. 2011. "Model-based Optimal Supervisory Control of Chilled Ceiling Displacement Ventilation System." *Energy and Buildings* 43: 1359–1370.
- Keblawi, A., N. Ghaddar, K. Ghali, and L. Jensen. 2009. "Chilled Ceiling Displacement Ventilation Design Charts Correlations to Employ in Optimized System Operation for Feasible Load Ranges." *Energy and Buildings* 41: 1155–1164.
- Keniar, K., K. Ghali, and N. Ghaddar. 2015. "Study of Solar Regenerated Membrane Desiccant System to Control Humidity and Decrease Energy Consumption in Office Spaces." *Applied Energy* 138: 121–132.
- Larson, M. 2006. "The Performance of Membranes in a Newly Proposed Runaround Heat and Moisture

- Exchanger.” M.Sc. thesis. University of Saskatchewan, Saskatoon. <http://library.usask.ca/theses/available/etd-12192006-094159/>.
- Mathworks. 2015. *MATLAB Version 8.5*. <http://www.mathworks.com/>.
- Mitchell, M. 1997. *An Introduction to Genetic Algorithm*. Cambridge: MIT Press.
- Mohammad, A. T., S. Bin Mat, M. Y. Sulaiman, K. Sopian, and A. A. Al-abidi. 2013. “Historical Review of Liquid Desiccant Evaporation Cooling Technology.” *Energy and Buildings* 67: 22–33.
- Mossolly, M., K. Ghali, and N. Ghaddar. 2009. “Optimal Control Strategy for a Multi-Zone Air Conditioning System Using a Genetic Algorithm.” *Energy* 34: 58–66.
- Mossolly, M., K. Ghali, N. Ghaddar, and L. Jensen. 2008. “Optimized Operation of Combined Chilled Ceiling Displacement Ventilation System Using Genetic Algorithm.” *ASHRAE Transactions* 114: 541–554.
- Mundt, E. 1996. “The Performance of Displacement Ventilation System.” PhD Thesis. Royal Institute of Technology, Sweden.
- Niu, J., L. Zhang, and H. Zuo. 2002. “Energy Savings Potential of Chilled-Ceiling Combined with a Desiccant Cooling in Hot and Humid Climates.” *Energy and Buildings* 34: 487–495.
- Novoselac, A., and J. Serbric. 2002. “A Critical Review on the Performance and Design of Combined Cooled Ceiling and Displacement Ventilation Systems.” *Energy and Buildings* 34: 497–509.
- Simonson, C. J., M. Salonvaara, and T. Ojanen. 2002. “The Effect of Structures on Indoor Humidity – Possibility to Improve Comfort and Perceived Air Quality.” *Indoor Air* 12: 243–251.
- Studak, J. W., and J. L. Peterson. 1988. “A Preliminary Evaluation of Alternative Liquid Desiccants for a Hybrid Desiccant Air Conditioner.” Proceedings of the Fifth Symposium on Improving Building Systems in Hot and Humid Climates. Houston, TX, September 12–14.
- Vashistha, V., and P. Talukdar. 2013. “Numerical Studies for Performance Evaluation of a Permeable Ceiling Panel for Regulation of Indoor Humidity.” *Energy and Buildings* 62: 158–165.
- Wang, X., W. Cai, J. Lu, Y. Sun, and X. Ding. 2013. “Hybrid Dehumidifier Model for Real-time Performance Monitoring, Control and Optimization in Liquid Desiccant Dehumidification System.” *Applied Energy* 111: 449–455.
- Wang, S., and X. Jin. 2000. “Model-based Optimal Control of VAV Air-conditioning System Using Genetic Algorithm.” *Building and Environment* 35: 471–487.
- Wang, N., J. Zhang, and X. Xia. 2013. “Desiccant Wheel Thermal Performance Modeling for Indoor Humidity Optimal Control.” *Applied Energy* 112: 999–1005.
- Woods, J. 2014. “Membrane Processes for Heating, Ventilation, and Air Conditioning.” *Renewable and Sustainable Energy Reviews* 33: 290–304.
- Xiao, F., G. Gaoming, and N. Xiaofeng. 2011. “Control Performance of a Dedicated Outdoor Air System Adopting Liquid Desiccant Dehumidification.” *Applied Energy* 88 (1): 143–149.
- Yuan, X., Q. Chen, and L. Glicksman. 2001. “A Critical Review of Displacement Ventilation.” *ASHRAE Transactions* 104 (1): 78–90.